Heliyon 10 (2024) e38113

Contents lists available at ScienceDirect

Heliyon

journal homepage: www.cell.com/heliyon

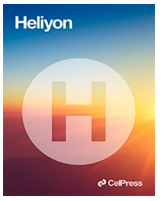

Research article

Microstimulation-based path tracking control of pigeon robots through parameter adaptive strategy

Yinggang Huang [a,b], Lifang Yang [a,b], Long Yang [a,b], Zehua Xu [a,b], Mengmeng Li [a,b,**], Zhigang Shang [a,b,*]

[a] School of Electrical and Information Engineering, Zhengzhou University, Zhengzhou 450001, China
[b] Henan Key Laboratory of Brain Science and Brain-Computer Interface Technology, Zhengzhou 450001, China

ARTICLE INFO

Keywords:
Pigeon robot
Stimulus model
Parameter adaptive strategy
Path tracking control
Behavioral pre-control

ABSTRACT

Research on animal robots utilizing neural electrical stimulation is a significant focus within the field of neuro-control, though precise behavior control remains challenging. This study proposes a parameter-adaptive strategy to achieve accurate path tracking. First, the mapping relationship between neural electrical stimulation parameters and corresponding behavioral responses is comprehensively quantified. Next, adjustment rules related to the parameter-adaptive control strategy are established to dynamically generate different stimulation patterns. A parameter-adaptive path tracking control strategy (PAPTCS), based on fuzzy control principles, is designed for the precise path tracking tasks of pigeon robots in open environments. The results indicate that altering stimulation parameter levels significantly affects turning angles, with higher UPN and PTN inducing changes in the pigeons' motion state. In experimental scenarios, the average control efficiency of this system was 82.165%. This study provides a reference method for the precise control of pigeon robot behavior, contributing to research on accurate target path tracking.

1. Introduction

The evolution of microelectronics and biomedical technology has given rise to a distinct category of animal robots, diverging from traditional robots. In this paradigm, animals replace mechanical structures, and neuroelectric stimulation serves as a control command transmitted to the sensory or motor cortex, enabling the manipulation of specific behaviors. This synthesis capitalizes on the inherent locomotion capabilities of animals while addressing energy supply challenges [1]. The research scope of animal robots encompasses water, land, and air domains [2], spanning behavioral interventions in mammals [3–7], fish [8], insects [9–11], and birds [12]. In particular, pigeon robots have garnered significant attention due to their natural advantages including a broad range of activities, low energy consumption, and superior covert performance. Currently, the primary control approaches for pigeon robots include the active and passive types. The active method involves stimulating the upward neural pathway, prompting the animal's brain to actively respond to external sensory information. On the other hand, the passive method stimulates the downward neural pathway, inducing the animal to passively respond to external neural stimuli. Notably, the passive approach is predominantly employed to stimulate the

* Corresponding author. School of Electrical and Information Engineering, Zhengzhou University, Zhengzhou, 450001, China.
** Corresponding author. School of Electrical and Information Engineering, Zhengzhou University, Zhengzhou, 450001, China.
E-mail addresses: limengmeng@zzu.edu.cn (M. Li), zhigang_shang@zzu.edu.cn (Z. Shang).

https://doi.org/10.1016/j.heliyon.2024.e38113
Received 22 February 2024; Received in revised form 12 September 2024; Accepted 18 September 2024
Available online 19 September 2024

motor executive brain area or muscle, which has been demonstrated as a reproducible and highly stable approach in existing research [13].

Studies have demonstrated the feasibility of utilizing passive stimulation modalities to target specific motor brain areas in pigeons, thereby controlling distinct motions [14]. Cai et al. [15] induced lateral rotation by applying stimulation to the formation of reticular medialis mesencephalic (FRM) in both free-roaming and anesthetized states. Jang et al. [16] proposed a correlation between the spatial location of the stimulus and the specific response of pigeons. They observed that positioning the stimulus site closer to the FRM nucleus, particularly when situated deeper in the ICo nucleus, resulted in lateral body motions rather than wing fluttering or forward walking when a high current stimulus was applied. Furthermore, they suggested that nuclei such as the tractus occipito-mesencephalicus (OM), nucleus rotundus (RT), and nucleus taeniae (TN) could induce rotation in pigeons. Nevertheless, the distinction between left and right brain areas was not explored, necessitating further investigation into behavioral reproducibility. Furthermore, stimulation of the right and left FRM during the pigeon's stable flight demonstrated effective flight rotation control with a wireless stimulator, localization module, and memory card attached to the pigeon's back [17,18]. Collectively, these studies affirm the consistent inducibility of rotation in pigeons through the stimulation of the FRM both on the ground and during flight [19–22].

Current neuroregulation methods include deep brain stimulation (DBS) [23], transcranial electrical stimulation (tES) [24], transcranial magnetic stimulation (TMS) [25], optogenetics [26], and ultrasound stimulation. Among these, neural electrical stimulation stands out as the dominant technique in animal robot control research, due to its rapid response, high stability, and excellent reproducibility. In the domain of neuroelectric stimulation, robust electrical stimulation is typically employed to ensure a reliable response. The primary used neural signal is a constant-current, cathode-fronted biphasic square wave [7,11,14,27]. Alternating positive and negative pulses maintain input charge balance in the brain and possess the capability to induce profound neural excitation, becoming a widespread application in the field of bioelectrical stimulation [28]. For instance, robotic insects achieve precise control over movement, turning, and flight through electrical stimulation of muscle groups and sensory systems within the brain or thoracic ganglia [29,30]. Similarly, electrical stimulation of specific brain regions in rats, such as the medial forebrain bundle (MFB), primary somatosensory cortex barrel field (S1BF), and superior colliculus (SC), effectively induces corresponding behaviors, enabling controlled forward movement and directional turns in robotic rats [31,32]. Likewise, stimulating the sensory cortex of carp results in left and right turns, demonstrating the potential for external control over biological movement behaviors [33].

Research on the behavioral regulation of bio-robots has demonstrated that organisms can respond to deep brain stimulation patterns to perform specific movements. It has been observed across different species that the success rate of behavior control can be significantly enhanced by flexibly configuring stimulation parameters. Additionally, it has been proven that external information, when encoded through electrical stimulation and transmitted to motor execution brain regions, can reliably induce behavioral responses.

While neuroelectric stimulation can be used for encoding sensory information that the central nervous system translates into corresponding motor outputs, excessive electrical stimulation may compromise the effectiveness of behavioral responses and lead to neuronal inactivation [34]. Consequently, a thorough investigation into the interplay between parameters such as pulse amplitude, duration, frequency, and pulse number becomes imperative to achieve precise control of animal robots. Currently, the predominant approach for analyzing these relationships is the control variable method, followed by the selection of an optimal parameter set to guide the pigeon robot in tracking a predefined path [35–37]. Zhao et al. [27] emphasized the interaction among stimulation parameters, highlighting the necessity of considering the interplay between different parameters in control. Fang et al. [38] further categorized stimulation parameters into four levels and employed sequential stimulation to quantify their impact on rotation behavior, achieving a precise division of the pigeon flight's rotation angle. Zhou et al. successfully employed a wireless neural stimulator to manually control a pigeon robot, tracking various directional paths in an indoor open setting [39]. Additionally, the effectiveness of neuromodulated pulses depends not only on the mentioned parameters but also on the stimulation mode [40]. Given that electrical stimulation signals can only mimic neural action potentials through preset unit signals, maintaining consistency with biological neural signal characteristics is challenging. Adopting a single pulse pattern may result in animal tolerance, reduced control duration, and the failure to ensure simultaneous activation of neurons [41]. Combining different pulse patterns into multiple stimulation modes can mitigate these issues, with no significant distinction observed between the right and left brain [17]. Yan et al. [42] investigated stimulation modes using simulated biological neural signals as stimulation output waveforms. Yang et al. [37] demonstrated that high-frequency multi-pulse stimulation modes consistently exert robust control over pigeons under prolonged stimulation states.

Previous studies on the optimal stimulation parameters and patterns for controlling the movement of pigeon robots have indicated that the integration of multiple pulse modes is more effective in meeting the complex demands of animal behavior control. However, these studies have not accounted for the varying rotational requirements at different moments during the control task, which can lead to overcorrection and cause the subject to sway back and forth along the target path, resulting in an "8" path. In recent years, this issue has been addressed by adjusting stimulation patterns to guide and control rat robots in performing corresponding movements and successfully developing an autonomous navigation system for rat robots [43]. Nevertheless, the development of autonomous control systems for flight-capable bio-robots remains an area that requires further exploration.

Therefore, establishing a real-time parameter-adaptive control algorithm is essential for accomplishing complex path tracking tasks in pigeon robots. Addressing the limitations of single stimulation mode control, which fails to meet the adaptive requirements of dynamic systems, this paper proposes a parameter-adaptive control strategy for pigeon robot path tracking. A feedback control system based on fuzzy control principles has been designed to enable precise tracking of target paths by pigeon robots in open environments. To implement this autonomous control system, the movement state must first be detected. This involves using target region segmentation techniques to locate the pigeon robot and calculate real-time position errors and their trends. Next, by analyzing the mapping relationship between parameter levels and behavioral responses, a parameter-adaptive path tracking control strategy is

formulated. Finally, output parameters are dynamically adjusted based on the control requirements at different stages of the task, with diverse stimulation modes employed to achieve precise and prolonged control of pigeon behavior. The proposed parameter-adaptive path tracking control strategydemonstrated exceptional navigation performance in a bidirectional open-field environment.

2. Materials and methods

2.1. Animals

In this study, seven adult pigeons (Ph1, Ph2, Ph3, Ph5, Ph7, Ph9, Ph10) with an average age of 2 ± 0.3 years and a body weight exceeding 400 g were selected. Both male and female pigeons were included. The pigeons were housed individually in wire cages under normal light-dark conditions, with free access to water, nutrient-rich soil, and a mixed diet. All animal experiments described in this paper were reviewed and approved by the Life Sciences Ethics Review Committee of Zhengzhou University (No. SYXK 2019–0002), in compliance with the guidelines set forth by the Institutional Animal Care and Use Committee (IACUC).

2.2. Experimental site and pre-training

A bidirectional open test field, measuring 2.7 × 1.8 m, was used in this study, as shown in Fig. 1a. Both sides of the field were enclosed with shade cloth to ensure a controlled environment free from human interference during the experiments. A Logitech C930e camera is positioned at the center of the site to capture experimental events. The target paths, illustrated as dotted lines in Fig. 1a, consist of a 1.7 m longitudinal path (Path 1), a 1.4 m lateral path (Path 2), and a 0.9 m longitudinal path (Path 3), with a total length of 4.1 m. Additionally, an opaque barrier measuring 0.7 × 0.1 × 0.005 m was strategically placed at the turning points.

The neuromodulation phase is preceded by 3–5 days of forward training. Pigeons underwent a period of food deprivation exceeding 24 h, and water, food, and nutrient soil were positioned at the end of the field. The feeding site served for rationing, with 2 g of food administered at a time. Upon their initial arrival at the feeding site, pigeons were relocated to the starting point. During this phase, they foraged and returned to the starting point undisturbed. This pre-training process instills in them the motivation to walk forward. This training methodology proves highly effective in control experiments, as it allows the animals to return to the starting point undisturbed, thus minimizing stress from external factors and enhancing their capacity for autonomous decision-making.

2.3. Surgery and targeted brain area

First, the pigeons were anesthetized with an intraperitoneal injection of 3% sodium pentobarbital (0.14 ml/100 g). Once the anesthesia took effect, the feathers on the head were shaved, and 2% lidocaine (0.2–0.3 ml) was administered subcutaneously for local anesthesia. The pigeons were then secured in a specially designed stereotaxic apparatus (Model 68027, RWD Life Sciences, Shenzhen, China), and the FRM region (AP: 3.90 mm, ML: 1.45 mm, DP: 8.0 mm) was selected as the implantation site based on the pigeon brain atlas (Karten and Hodos, 1967). The brain region is illustrated in Fig. 2. A cranial drill was used to remove a piece of skull (3 mm × 3 mm) to expose the brain tissue. After exposing the dura mater, a single electrode (100 μm diameter nichrome stainless steel wire, PTFE insulated) was implanted. Ear brain gel was applied as a buffer between the brain and dental cement. Two screws were implanted in the skull, and after inserting the two electrode wires, silver wire was wound around the screws as a reference electrode. All electrode implantation sites were sealed with α-cyanoacrylate quick medical adhesive to close the gaps between the screws and the skull. The electrode connector was then secured with dental acrylic resin. A 5% enrofloxacin solution was applied to the surgical area for disinfection and to prevent inflammation. During the recovery period, the birds were housed individually in wire cages (70 × 50 × 50 cm), with access to food and water for 7 days, and the surgical area was cleaned regularly. Fig. 1b shows a pigeon robot wearing a wireless neural stimulator after surgical recovery.

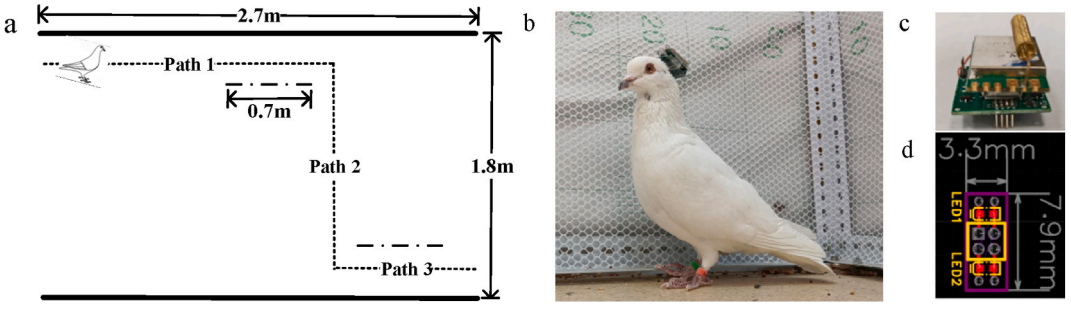

Fig. 1. Experimental model design and pigeon robots. (a) Schematic diagram of the experimental site. (b) Experiment with a pigeon robot wearing a wireless neurostimulator. (c) Wireless neurostimulator. (d) Electrode converter PCB circuit diagram.

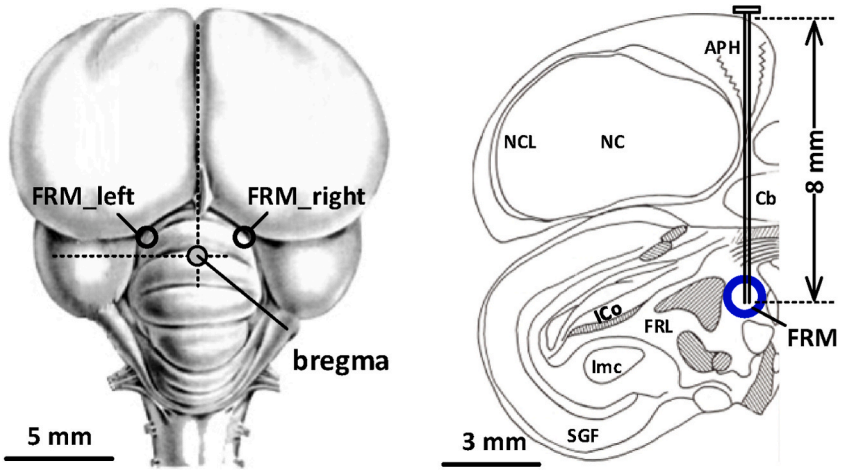

Fig. 2. Schematic of FRM Brain Region Stimulation Electrode Implantation. (a) Anatomical diagram of the pigeon brain. (b) Localization of the FRM brain region.

2.4. Wireless neurostimulator and electrode converter

The wireless neural stimulator from the literature reference [27] was upgraded, with the stimulation module being controlled by a microcontroller (C8051F020) to regulate current output. This setup ensures the stable generation of a constant current ranging from 5 to 0.7 mA, with a frequency range of 25 Hz to 10 kHz. The stimulation parameters include the number of pulse trains (1–255), the number of pulses per train (1–255), and the interval between pulse trains (0.1–25.5 s). A radio frequency (RF) communication module was used to establish point-to-point data connectivity with the host computer. The device measures 3.3 × 2.4 × 1.5 cm and weighs 7.9 g (including a 100 mAh battery), with an operational duration of approximately 70 min. The wireless neural stimulator is depicted in Fig. 1c.

The stimulator output pulse was configured as a biphasic constant-current square wave with cathodic precession, maintaining a total charge output of zero. This design aimed to alleviate the adverse effects of DC stimulation on the target nucleus, ensuring that bi-

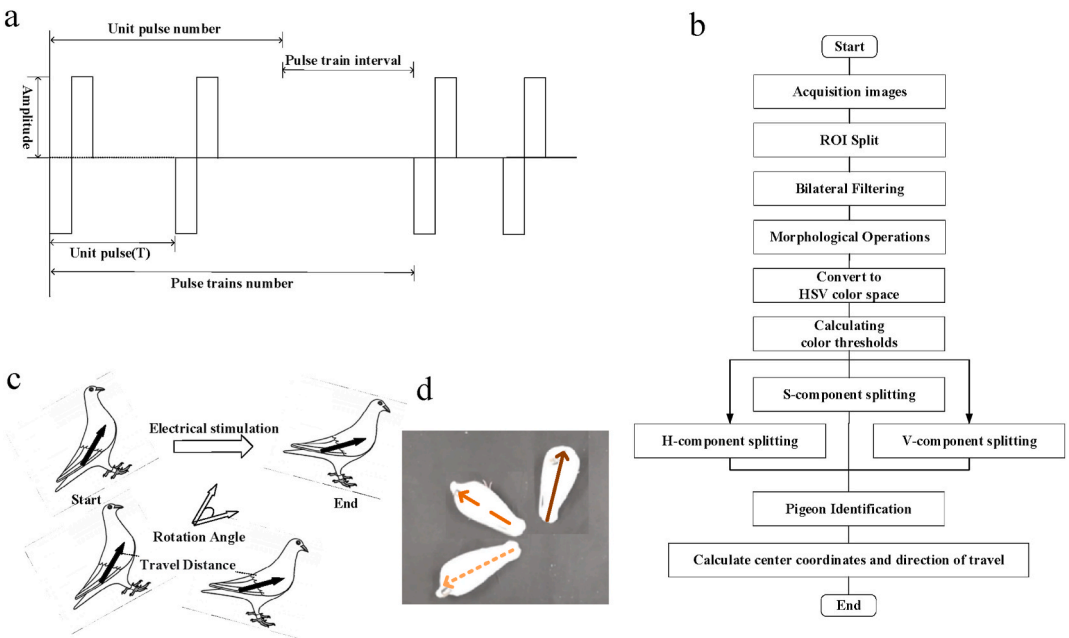

Fig. 3. Wireless neurostimulator basic output waveform and pigeon motion state identification. (a) Schematic diagram of modulated pulses. (b) Flow chart of pigeon motion status recognition based on HSV color space method. (c) Calculation method of rotation angle and motion distance. The black arrow represents the current body direction of the pigeon, the angle between the hollow arrows is the steering angle before and after electrical stimulation, and the distance between the center of gravity of the pigeon's body is the travel distance before and after electrical stimulation.

directional pulses did not introduce charge bias within or outside the neuronal membrane [44]. To mitigate the risk of electrode displacement due to prolonged exposure of electrode wires outside the body, a 4-channel electrode converter was developed. Each channel of this converter connects individually to a deep brain stimulation electrode and a reference electrode positioned on the skull's surface. A 2x2 female header located at the top is used to connect to the output port of an external stimulator, as illustrated in Fig. 1d. The device is constructed from a printed circuit board (PCB), LEDs, and a dual-row 2x2 direct insertion bus, and is sealed with waterproof adhesive to ensure durability. A single stimulation electrode on each side, along with the corresponding skull reference electrode, was connected to the same side of the electrode converter, forming a current loop within the pigeon's brain. During electrical stimulation experiments, the LEDs were monitored to confirm the application of electrical stimulation signals. The impedance value of the device, measured using the impedance tester ni-POD (NeuroNexus Technology, USA), ranged from 0.03 to 0.09 MΩ.

2.5. Neuroelectrical stimulation parameters and stimulation modes

Neuroelectrical stimulation initiates a firing response in neurons through the delivery of an external electrical charge to the designated brain area, eliciting a shift in membrane potential. Neuroactivity is contingent on the cumulative charge imparted to the neural tissue, a value influenced by pulse parameters, stimulation modes, together with the electrode materials and implantation locations. Current research indicates that both higher stimulation intensity and longer stimulation duration have a greater impact on pigeon behavior, while more frequent single stimulations result in increased damage to brain tissue. Based on these findings, the primary stimulation parameters used in this study, as illustrated in Fig. 3a, include pulse frequency (PF/Hz), number of pulses per train (UPN/Size), number of pulse trains (PTN/String), and pulse amplitude (PA/mA). These parameters were selected to achieve neuro-control of pigeon robot behavior while ensuring biological safety.

1. PF: Defined as the number of pulse signal cycle changes per second, expressed as PF = 1/T, where T represents the time of the unit pulse cycle.
2. UPN: Refers to the quantity of unit pulses within a unit pulse sequence.
3. PTN: Indicates the count of unit pulses within a pulse sequence.
4. PA: Denotes the peak value of current per unit pulse.

In addition, we set the duty cycle (ρ) at 33% to control the pulse interval, which dictates the discharge duration of the neuro-modulated pulse. The pulse train interval (PTI) is standardized at 100 ms representing the time gap between pulse trains. According to previous studies, different brain tissue possesses a specific activation frequency [8], and the nervous system does not respond uniformly to arbitrary electrical stimulation frequencies [45]. Studies [18,19,36,38] indicate that the frequency of neuronal activation in the pigeon brain is primarily centered below 120 Hz. Therefore, the stimulation parameters used in this experiment are listed in Table 1.

All experiments quantifying the behavioral responses to stimulation parameters were conducted using the method of controlling variables. The increments for stimulation parameters were 25 Hz for frequency, 1 pulse for UPN, 1 train for PTN, and 0.1 mA for amplitude. To ensure the robustness of the behavioral control study, parameters that reliably induced behavior were established as initial values. The initial stimulation parameters, determined from post-surgical verification experiments, were 50 Hz for frequency, 4 pulses for UPN, 3 trains for PTN, and 0.2 mA for amplitude. To minimize the impact of sequential increments on statistical analysis, a pseudorandom sequence was used to determine the order of testing parameters. Each test focused on the effect of a single parameter on behavior, with neural stimulation repeated 10 times in the FRM brain regions of both the left and right sides of all subjects to ensure the reproducibility of behavioral induction.

To ensure the robustness of the behavioral control study, the parameters that could stabilize the evoked behavior were established as the initial values. The initial stimulation parameters derived from postoperative locus validity experiments were determined to be 0.2 mA, 50 Hz, 4 sizes, and 3 strings. All experiments were conducted using the controlled variable method and employed biphasic constant current pulse stimulation. The PF, UPN, PTN, and PA were then randomized for adjustment, with unit increments of 0.1 mA, 25 Hz, 1 size, and 1 string, respectively. Each set of trials focused on a single parameter and was repeated 10 times in both the right and left FRM of all subjects to ensure the reproducibility of effects. To mitigate the impact of sequence increment on statistical analysis results, a pseudo-randomized sequence was used to determine the order of the tested parameters.

Table 1
Parameter conditions used for experiments on the relationship between parameter levels and behavioral responses.

Waveform	Parameters	Unit	Range	Test level				Control	Increment
Bidirectional, positive, and negative square waves	PF	Hz	25–100	25	50	75	100	50	25
	UPN	size	3–6	3	4	5	6	4	1
	PTN	string	2–5	2	3	4	5	3	1
	PA	mA	0.2–0.5	0.2	0.3	0.4	0.5	0.3	0.1

2.6. Pigeon motion state recognition

Accurate and efficient detection methods will enhance the operational efficiency of the online control system. In this paper, we employ the HSV-based color space to extract the motion state of the pigeon robot [46]. The three components—H (hue), S (saturation), and V (value)—are independent of each other, with H and S being minimally affected by light and shadow occlusion. Fig. 3b illustrates the flowchart of pigeon motion state recognition based on the HSV color space. The variables of rotational angle (RA) and travel distance (TD) were introduced to quantitatively assess the effects of neural stimulation on the rotational control behavior of pigeon robots, as shown in Fig. 3c and 3d. Images of the pigeons were captured using a camera, and target area segmentation techniques were employed to extract images of the pigeon robot at the start and end of stimulation. These images were used to calculate RA and TD, thereby observing the relationship between different levels of stimulation parameters and their effects. This approach facilitates a quantitative evaluation of the behavioral responses. In this study, the pigeon's movement states were categorized into three types: stationary, rotational, and walking. Transitions between states, which are generally associated with body movement, were quantified using a step count metric.

2.7. Analysis of behavioral variability at different parameter levels

To assess the significance among different parameter levels inducing rotation behaviors (as presented in Table 1), the rotation angle and distance traveled were computed for each level. The test results were then presented as mean ± standard error (SE). Statistical analyses were performed using SPSS 27.0 software, and the normality and homogeneity of the variance were assessed using the Shapiro-Wilk W-test and Levene's test, respectively.

Each parameter level was iterated 10 times in both the left and right brain areas of each subject. Analysis of variance (ANOVA) was conducted to explore variances between individual rotation behaviors and parameter settings, with the significance level set at 5% (*, $p < 0.05$). LSD post hoc analysis was employed to examine the impact of parameter level selection on rotation behavior [47]. In instances of variance nonuniformity, the Broen-Forsythe test and Tamhane's T2 post hoc analysis were used for significance analysis and pairwise comparisons, respectively.

2.8. Parameter-adaptive path tracking control strategy

Pigeons can autonomously determine their behavior based on the environmental context. Pigeons usually exhibit specific behaviors by their inherent motion patterns, deviating from our expectations if the deviation from the target path is not suppressed. Consequently, the automatic navigation system of animal robots exhibits significant randomness. The use of a parameter-adaptive path tracking control strategy allows for pre-adjustment of the pigeon's motion path. This helps in restraining impending transgressions or instances of control loss during the tracking. Furthermore, it will avoid path fluctuations caused by system hysteresis control. The fuzzy control algorithm does not rely on an accurate model of the controlled system and is capable of managing uncertain systems. Using this method, a path tracking control system for the pigeon robot was established, as illustrated in Fig. 4a. The camera captures the position information (x_p, y_p) of the pigeon robot during the feeding process, facilitating the computation of positional error (e) and the rate of

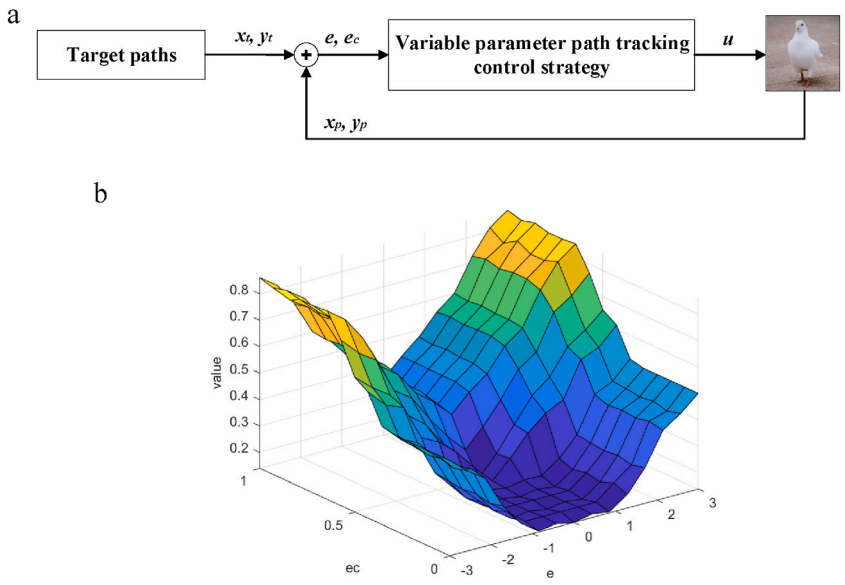

Fig. 4. Pigeon robot path tracking control system and strategy. (a) Design block diagram of pigeon robot path tracking control system. (b) parameter adaptive path tracking control strategy control rule.

change of the error (e_c) using Equation (1):

$$\begin{cases} e = \left(x_p, y_p\right) - (x_t, y_t) \\ e_c = (e_{t-1} - e_t)/\Delta t \end{cases} \tag{1}$$

Where x_t and y_t represent the reference coordinates of the target path, $e_{t\text{-}1}$ and e_t denote the positional error at the previous and current moments, respectively.

The positional information (x_p, y_p) acquired by the camera during the pigeon feeding process is used in the PAPTCS as a system state variable. This enables the real-time generation of a set of stimulation parameters, denoted as u, to fulfill the current tracking requirements. Subsequently, the wireless neural stimulator generates stimulation signals corresponding to the stimulation modes, transmitting them to the FRM via the electrode converter. This process achieves the functionality of automatic control of the pigeon robot's behavior.

To prevent tolerance development due to frequent electrical stimulation, errors within the pigeon's body width ($E = 10$ cm) are considered as within the target path, expressed as $|e| \leq E$. The selection rule for the *PA* parameter is determined by the following equation:

$$PA = V_{\min} + \beta(V_{\max} - V_{\min}) \tag{2}$$

Where $V_{\min}$ and $V_{\max}$ represent the minimum and maximum amplitude values, respectively; the adjustment factor β increases nonlinearly and monotonically with both the error e and the rate of change of the error e_c.

When $E \leq |e| \leq 2E$, the parameter selection rule is

$$\begin{cases} [\beta_L \quad UPN_L \quad PTN_L \quad PF_H], 0 < |e_c| < 0.3 \\ [\beta_M \quad UPN_M \quad PTN_M \quad PF_M], 0.3 \leq |e_c| \leq 0.7 \\ [\beta_M \quad UPN_H \quad PTN_M \quad PF_M], 0.7 < |e_c| \end{cases} \tag{3}$$

When $|e| > 2E$, the parameter selection rule is

$$\begin{cases} [\beta_M \quad UPN_M \quad PTN_M \quad PF_H], 0 < |e_c| < 0.3 \\ [\beta_M \quad UPN_H \quad PTN_M \quad PF_M], 0.3 \leq |e_c| \leq 0.7 \\ [\beta_H \quad UPN_H \quad PTN_M \quad PF_M], 0.7 < |e_c| \end{cases} \tag{4}$$

Where, *UPN*, *PTN*, and *PF* represent the values within the selected parameter ranges corresponding to different behavioral responses. L, M, and H denote the respective parameter levels within these ranges. Fig. 4b shows the fuzzy control rules.

2.9. Control strategy performance metrics

To comprehensively assess the control strategy's performance, two parameters are defined. The task-averaged error rate α evaluates the accuracy of the control strategy in tracking the target path, while the control efficiency η assesses the system's effectiveness in successful experimental trials. An efficiency level ($\eta > 70\%$) is considered the highly efficient control interval.

$$\alpha = \left(1 - \left(\sum_{i=1}^{n} (|e_i|) \Big/ n \Big/ E\right)\right) \times 100\% \tag{5}$$

$$\eta = \left(1 - \frac{T_c}{T}\right) \times 100\% \tag{6}$$

Where n represents the total number of samples in the experiment, T_c denotes the system control duration, T corresponds to the overall experiment duration, the value range of α is (-∞, 100%], and the value range of η is (0, 100%].

Statistical evaluation of system repeatability in multi-individual, multi-trial experiments is performed through the control efficiency (η) and the task-averaged error rate (α). Experimental success is determined based on two criteria.

1. Rapidity requirement: T should be less than 2 times the free foraging time (T_f) in the uncontrolled state.
2. Accuracy requirement: α between 0% and 100% fulfills the system's accuracy criterion for path tracking. When α is less than 0, the system loses its ability to control the pigeon robot.

The task is deemed successful when both conditions are met; otherwise, it is considered a failure. The duration taken to stabilize the foraging route during pre-training was recorded as the freely foraging time (T_f). Five pigeon robots (Ph1, Ph2, Ph5, Ph7, Ph10) participated in the experiment, and each individual underwent ten repetitions. Finally, both control efficiency (η) and task-averaged error rate (α) were calculated for each trial to facilitate statistical analysis.

3. Results

In this section, we analyze the impact of varied parameters on the motion behavior of pigeons within a two-way open field. Simultaneously, we discuss the tracking performance of the automatic control system. Our objective is to achieve the autonomous tracking of the pigeon robot along a predefined path in an open-field scenario and enhance tracking accuracy through PAPTCS. To ensure experiment reliability, pigeons undergo a fasting period exceeding 12 h before any test, ensuring their predominant forward momentum originates from food. Following each test, the experimental site undergoes meticulous cleaning, ventilation, and a half-hour drying period before subsequent experiments.

3.1. *The impact of Neuroelectrical stimulation patterns on the response actions and state switching*

The experiment successfully collected data from five pigeon robots, with the results illustrated in Fig. 5.

(1) Impact of PF/Hz on RA and TD

As the frequency increased from 25 Hz to 100 Hz, RA on the left side decreased from 144.55° to 77.52°, while TD decreased from 8.39 cm to 6.65 cm. A similar decreasing trend was observed on the right side, where RA decreased from 103.45° to 49.76° and TD from 10.26 cm to 6.57 cm. The increase in frequency led to a reduction in both RA and TD, suggesting that high-frequency stimulation may suppress the pigeon's response. Although the trends on both sides were similar, the RA and TD on the right side were smaller than those on the left. A strong positive correlation between RA and TD was observed on the left side ($r = 0.89$), but it was not statistically significant ($p = 0.11$, $p > 0.05$). On the right side, a very significant positive correlation was found between RA and TD ($r = 0.99$, $p = 0.013$, $p < 0.05$), indicating a higher level of synchronization under frequency variations.

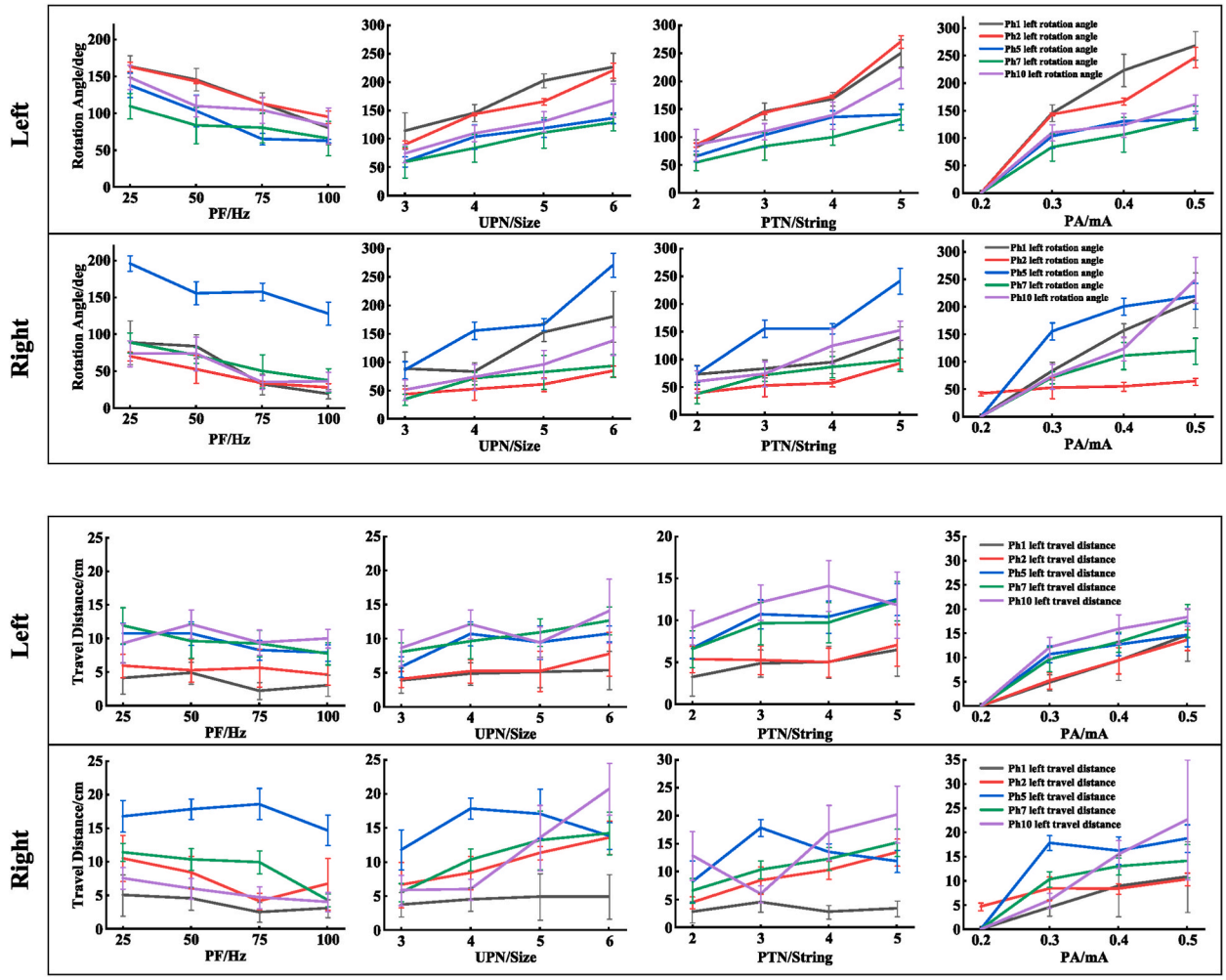

Fig. 5. Behavioral responses of individual subjects to different levels of stimulation parameters.

(2) Impact of UPN/Size on RA and TD

As the number of unit pulses increased from Size 3 to 6, both RA and TD increased on both sides. On the left side, RA increased from 79.49° to 175.87°, and TD increased from 6.12 cm to 10.12 cm. On the right side, RA increased from 60.92° to 153.14°, and TD from 6.74 cm to 13.44 cm. Although RA on the right side was slightly lower than on the left side, the increase in TD was more pronounced, indicating a more significant impact of pulse quantity on the right side. A strong positive correlation between RA and TD was observed on the left side ($r = 0.92$), but it was not statistically significant ($p = 0.081$, $p > 0.05$). On the right side, the positive correlation was stronger and significant ($r = 0.97$, $p = 0.033$, $p < 0.05$).

(3) Impact of PTN/String on RA and TD

As the number of pulse trains increased from 2 to 5, both RA and TD increased on both sides. On the left side, RA increased from 74.82° to 199.35°, and TD increased from 6.21 cm to 10.03 cm. On the right side, RA increased from 56.84° to 144.76°, and TD from 6.99 cm to 12.82 cm. A very strong and significant positive correlation between RA and TD was observed on both sides (Left: $r = 0.95$, $p = 0.047$; Right: $r = 0.98$, $p = 0.021$), indicating that the trend of influence due to the number of pulse trains is consistent across both sides, with a greater magnitude of change on the right side.

(4) Impact of PA/mA on RA and TD

With increasing amplitude, both RA and TD showed significant increases on both sides. On the left side, RA increased from 8.48° to 189.27°, and TD from 0 cm to 15.77 cm. On the right side, RA increased from 0° (no response) to 172.72°, and TD from 0.94 cm to 15.33 cm. A very strong and highly significant positive correlation between RA and TD was observed on both sides (Left: $r = 0.99$, $p = 0.007$; Right: $r = 0.99$, $p = 0.011$), demonstrating that changes in amplitude can precisely control the pigeon's motor responses.

Next, a detailed analysis of the relationship between stimulation parameters and behavioral responses will be provided using the Ph2 individual as an example.

A detailed analysis is provided using stimulation of the left FRM brain region in the Ph2 individual as an example.

Table 2 presents the statistical outcomes of the behavioral responses to the left FRM stimulation in Ph2. Each set of parameter levels corresponds to 10 experiments, and the results are expressed as mean ± standard deviation.

The extent of motion response in pigeons exhibited a direct correlation with the stimulus parameters, as illustrated in Fig. 6. Keeping other parameters constant, a negative correlation was observed between the rotation angle and PF (Fig. 6a, $p < 0.001$, Tamhane's T2 test). Conversely, there was no significant difference between travel distance and PF (Fig. 6b, $p > 0.05$, Tamhane's T2 test). Specifically, a high frequency of 100 Hz (PF = 100 Hz) induced the pigeon robot to execute a lateral rotation of approximately 90°, prompting the body to laterally advance by 1 or 2 steps during rotation, thereby achieving effective locomotor rotation. These results indicated that PF played a crucial role in control rotation with smooth and coherent response motions (Fig. 6c).

It was observed that the parameters UPN and PTN significantly influenced the RA (Fig. 6d for UPN, $p < 0.001$, Tamhane's T2 test; Fig. 6g for PTN, $p < 0.001$, Tamhane's T2 test). An increase in UPN and PTN in the stimulus pattern led to a behavioral response pattern opposite to that observed with PF. Notably, a distinct state switch was observed when UPN = 6 or PTN >4. Under these conditions, pigeons swiftly transitioned from a stationary state to a walking state in three steps, completing a rapid sideways rotation (Fig. 6f and 6i). Changes in UPN exhibited a weak correlation with travel distance (Fig. 6e, size = 3 and 6, $p = 0.045$, Tamhane's T2 test). Similarly, the variability between different levels of PTN and TD was modest (Fig. 6h, string = 4 and 5, $p = 0.03$, LSD test). However, an increase in PTN and UPN prolonged the duration of the neuromodulation process, allowing for an upper limit of rotation angle control of approximately 200°.

Table 2
Results of pigeon motion and behavior stimulated by different parameters.

Parameter		Travel Distance	Rotation Angle	Behavioral Response
PF/Hz	25	5.9353 ± 1.7457	162.7904 ± 6.3676	3 step rotation
	50	5.2609 ± 1.6975	143.4492 ± 2.5180	2 step rotation
	75	5.6460 ± 2.7993	113.1822 ± 8.4340	1 or 2-step rotation
	100	4.5979 ± 1.5305	95.0570 ± 8.4330	1 or 2-step rotation
UPN/size	3	4.0800 ± 1.1804	90.0169 ± 6.6203	1 step rotation
	4	5.2609 ± 1.6975	143.4492 ± 2.5180	2 step rotation
	5	5.2615 ± 2.9453	165.6477 ± 5.7185	2 step rotation
	6	7.7657 ± 30.2148	220.2573 ± 13.5859	3 steps rotation and walk
PTN/string	2	5.3714 ± 1.5710	85.9889 ± 3.8514	1 or 2-step rotation
	3	5.2609 ± 1.6975	143.4492 ± 2.5180	2 step rotation
	4	5.0112 ± 1.7234	172.8702 ± 2.8924	2 steps rotation and walk
	5	7.0360 ± 2.4832	270.2296 ± 10.9783	3 steps rotation and walk
PA/mA	0.2	0	0	stationary state
	0.3	5.2609 ± 1.6975	143.4492 ± 2.5180	2 step rotation
	0.4	9.3989 ± 2.7225	166.9253 ± 6.0240	2-step quick rotation
	0.5	13.6170 ± 2.1177	246.5010 ± 18.7035	3-step rotation, off balance

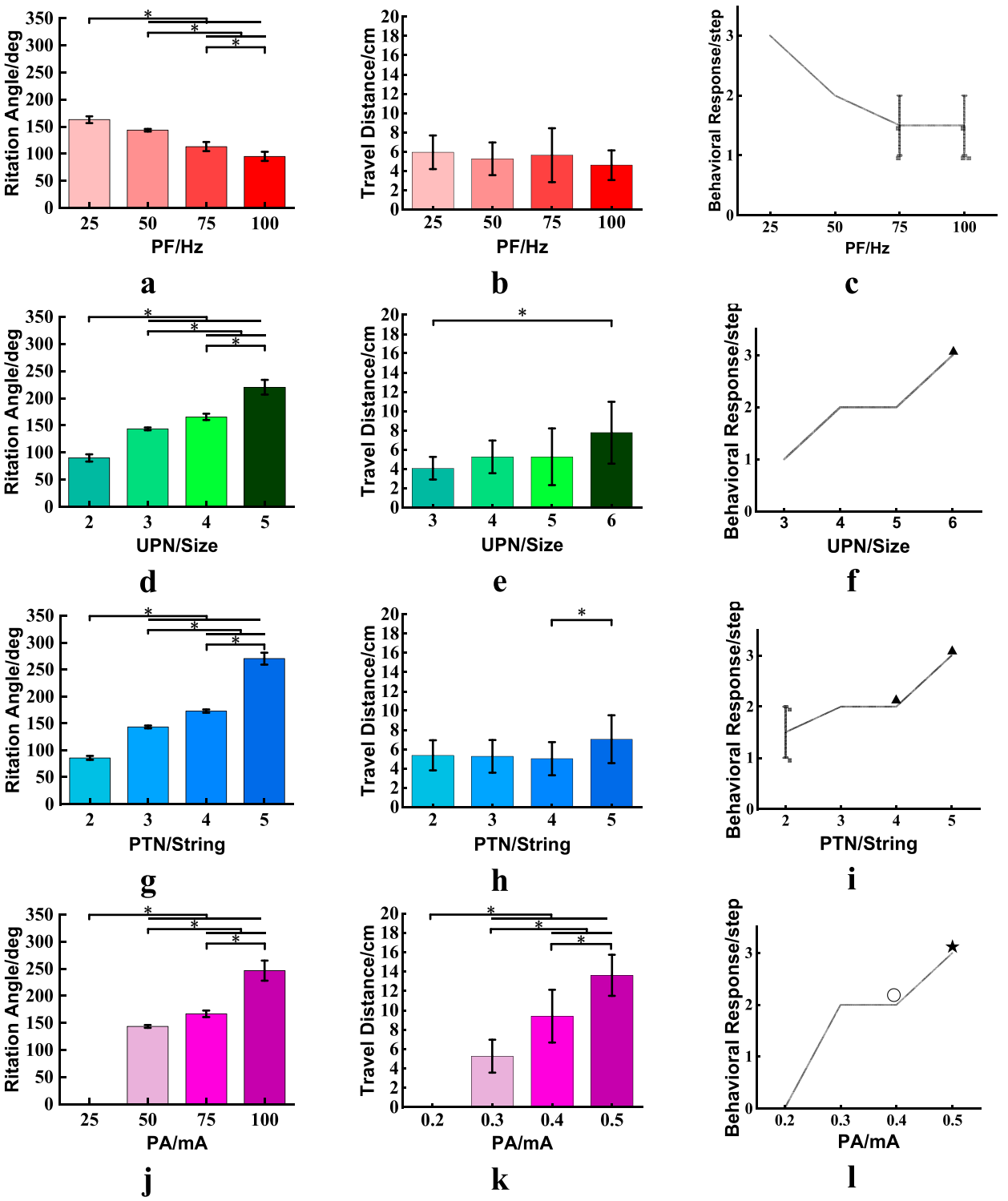

(caption on next page)

Fig. 6. The degree to which different stimulus parameters changed the locomotion state of pigeons. (a, b, c) Represent rotation Angle, motion distance, and behavioral response under different levels of stimulus parameter PF, respectively. (d, e, f) Represent rotation Angle, motion distance, and behavioral response under different levels of stimulus parameter UPN, respectively. (g, h, i) Represent the rotation Angle, motion distance, and behavioral response under different levels of stimulus parameter PTN. (j, k, l) Represent the rotation Angle, motion distance, and behavioral response under different levels of stimulus parameter PA, respectively. The thick black lines in Figs. j, k, and l indicate that all trials are generated stably; the rectangular boxes indicate the range of state switching for all trials.
Note: * indicates that there is significance between the two (*, $p < 0.05$). ▲ represents that the pigeon switches from a stationary state to a walking state at the end of the motion; ⚬ represents that the pigeon responds quickly and moves rapidly; ★ represents that the pigeon loses its body balance at the end of the motion.

PA exhibited a positive correlation with both RA and TD. In contrast to the other parameters, PA displayed a distinctive “threshold" for behavior control, beyond which the pigeon robot initiated behavioral responses. Notably, both RA and TD showed significant increases at PA = 0.3, with angular increments strongly correlated with PA increments (Fig. 6j for RA, $p < 0.001$, Tamhane’s T2 test; Fig. 6k for TD, $p < 0.001$, Tamhane’s T2 test). Higher PAs resulted in shortened response times, and larger PAs led to quicker and more vigorous motions. Specifically, at PA = 0.4 mA, the pigeons exhibited sharp, unsteady rotation, swiftly adjusting their body balance after the rotation. At PA = 0.5 mA, the pigeons executed three rapid lateral rotations and reached a rotation angle of about 250°. However, this rapid response led to a gravity center loss, indicating that higher PAs are relatively less effective in control rotation angles (Fig. 6l).

3.2. Experiments on PAPTCS for Pigeon robots

The average success rate across the five individuals was 78%, with Ph2 achieving the highest success rate of 90%, while Ph10 had a success rate of 60%. Table 3 presents the statistical results for all individuals in the path tracking experiments. Out of 50 trials, a total of 11 failures were observed, with 5 instances failing to meet speed requirements and 7 instances failing to meet accuracy requirements.

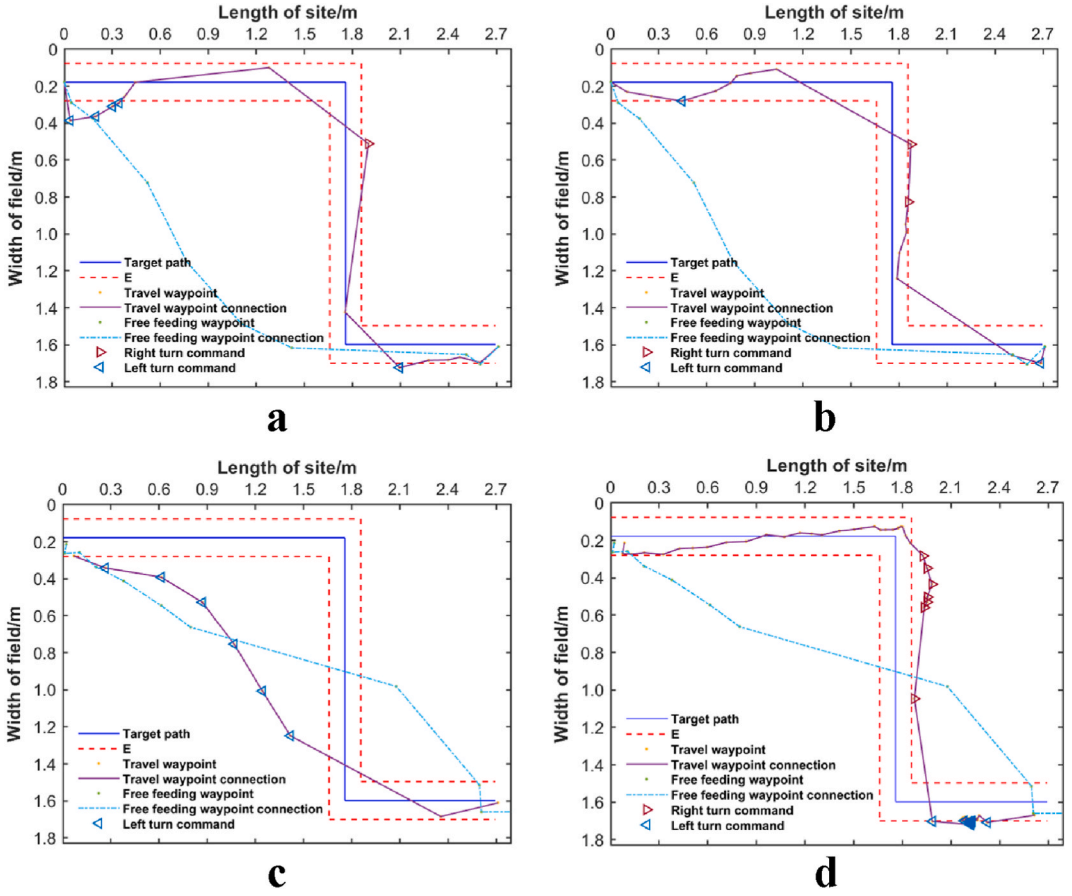

Fig. 7. The tracking effect of PAPTCS on complex paths. (a) Path tracking effect of successful trial 2. (b) Path tracking effect of successful trial 5. (c) Path tracking effect on failed trials, accuracy did not meet system design requirements. (d) Path tracking effect on failed trials, rapidity did not meet system design requirements.

Table 3
Number of crossing times of the second route. Note: The first two out of ten experiments of the pigeon robot Ph1 were failed attempts, so only attempts 3–10 were counted.

Test	3	4	5	6	7	8	9	10
N_2/N	7/8	6/7	7/8	4/6	3/4	4/5	2/2	6/6

Notably, Ph10 met both accuracy and speed requirements in its sixth trial. The subsequent analysis will provide a detailed examination of the path tracking control performance of the PAPTCS.

The results of trial 2 for pigeon Ph7 are depicted in Fig. 7a, where a total of 6 self-control commands were administered. The average error rate (α) of the task was calculated as 13.8542%, and the total experiment duration $T = 11.0326$s, affirming the success of the trial with an efficiency score (η) of 62.5%. The pigeon robot, endowed with autonomous path selection capabilities, instinctively followed the pre-training route upon leaving the nest. However, deviations from the predetermined target path occurred, evident by a detected position error $e = 20.4167$ cm at the second point, showcasing a trend of continuous increment. To rectify this deviation, the system applied left turn commands with varied stimulus patterns. Deviation from the target path was observed at every corner. By PAPTCS, frequency reduction was employed to counteract external intervention tendencies, progressively guiding the pigeon robots back to the target path, ultimately accomplishing the tracking task.

Fig. 7b depicts the outcomes of Trial 5 for pigeon Ph7, where the deviating from the prescribed path was detected four times. In each case, timely corrections were applied to the travel direction, ensuring the completion of the tracking task within the specified time frame through intervention in the behavioral decision-making of the pigeon robot. The average error rate $\alpha = 37.7451\%$, fulfilled the accuracy requirement. The experimental duration of 11.3936s, being less than $2T_f$, also met the rapidity criterion. Moreover, the control efficiency (η) at 76.4706% surpasses the 70% benchmark, aligning with the system's design goal for precise tracking.

Task failure can arise from two scenarios. The first one is depicted in Fig. 7c, typically observed at the experiment's onset. The pigeon's capacity to memorize its inherent feeding route plays a role when the cumulative charge of the system's applied stimulus modes lacks the potency to suppress the neuronal firing activity initiated by its consciousness. In such instances, the pigeon robot proceeds directly to the foraging site. Despite meeting the rapidity requirement, this trial falls short of fulfilling the system's accuracy standard, resulting in task failure.

Another scenario is depicted in Fig. 7d when the pigeon robot transitions from Path 1 to Path2. The deviance between the route autonomously selected by the pigeon robot according to the visual information from the foraging place and the expected direction would result in a state of hesitation and locomotor decision delays (i.e., (x_p, y_p)=(1.8, 0.18)). Upon reevaluation, the pigeon tended to proceed along a straight line toward the foraging site, leading to five transgressions at 0.2–0.6 m along Path2. The system intervened to curb the escalating error, enabling a return to the target path. However, interference from its visual afferent information caused a renewed deviation at $y_p = 1.0$m. Consequently, the system persisted in applying neuroelectric stimulation to govern the generation of right-turn behavior and adjust the forward direction until reaching the foraging site. Despite an accuracy-compliant $\alpha = 11.2538\%$, the experimental time $T = 138.2109$ s exceeded $2T_f$ (118.2149 s), resulting in task failure.

Table 4 presents the statistical results of the instances (N_2) where Ph1 crossed the boundary of Path2. The pigeon robot can observe the food and water directly in this path, frequently leading to a straight walk to the foraging ground. So the configuration of Path2 contradicts the pigeon's intended test path, making it a crucial indicator of the control system's performance. When the desired forward direction aligns with the free-foraging direction and facilitates progress toward the destination, significant deviations from the intended path become less likely. However, controlling the robot to adhere to the target path becomes challenging in situations where the angle between the pigeon robot's desired travel direction and the free foraging direction is approximately 90° (as depicted in the Path2 segment of Fig. 7). During such instances, the pigeon robot's neural activity experiences a substantial surge, posing a risk of task failure without adaptive adjustment of stimulus modes. Conversely, the PAPTCS simulating the relationship between individual parameter levels and behavioral responses, dynamically adapts stimulus parameter outputs based on system state quantities at different moments, ensuring the control system's adaptability under diverse conditions.

Table 4
Variable parameter control policy parameter.

Pixel position	position error e	Rate of position error change e_c	PA	UPN	PTN	PF
(1165,217)	**15.9**	**53.06%**	**0.37**	**2**	**2**	**61**
(1203.5324)	**22.3**	**74.44%**	**0.41**	**3**	**2**	**56**
(1192.5411.5)	**20.5**	**68.33%**	**0.41**	**3**	**2**	**58**
(1158,509)	**14.7**	**49.17%**	**0.36**	**2**	**2**	**62**
(1577.5,1031)	14.66	48.89%	0.36	2	2	62
(1583.5,1021.5)	13.1	43.61%	0.35	2	2	68

Note: The bolded portion of the table shows the state quantities and neuromodulation pulse parameters of the pigeon robot in the Path 2 section.

Table 5
Performance indexes of parameter-adaptive path tracking control strategy.

Individual Value Test		1	2	3	4	5	6	7	8	9	10	η_e	α_e	Success rate
Ph1	η	84.0909	90.411	71.4286	74.0741	70.3704	78.5714	82.6087	77.2727	92.8571	77.7778	74.0741%	36.7675%	80%
	α	36.0606	11.2538	18.6607	24.784	20.3704	39.494	55.0362	47.9924	59.3452	28.4568			
	T	***43.6044***	***138.2109***	17.331	15.0544	16.6191	17.2417	12.7844	12.3168	14.3864	17.9228			
	T_f			19.996			T_e			15.4571				
Ph2	η	33.3333	43.75	86.3636	78.9474	80	84.2105	100	83.3333	88.2353	90.3226	81.6847%	32.9263%	90%
	α	***-269.9074***	4.0625	42.9545	6.9737	28	37.193	61.6912	28.6574	37.7451	49.0591			
	T	9.5144	16.0941	12.206	12.3059	14.218	10.7397	13.8725	10.8216	9.3312	17.3688			
	T_f			27.5662			T_e			12.9953				
Ph5	η	50	66.6667	81.25	70	81.8182	86.3636	94.4444	77.7778	88.2353	69.2308	81.14%	34.0367%	80%
	α	***-9.6429***	20.5952	35.8333	21	29.0909	54.8485	39.4907	22.7315	38.5294	30.7692			
	T	14.6401	***15.7364***	11.7733	14.2799	11.2629	14.2179	11.1045	12.6382	9.984	10.4641			
	T_f			15.034			T_e			11.9656				
Ph7	η	46.1538	62.5	96	85	76.4706	97.1429	95	97.1429	81.8182	50	93.1577%	41.3411%	80%
	α	***-267.2436***	13.8542	50.0667	33.1667	37.7451	55.1667	45.7708	56.0952	38.8636	***-22.123***			
	T	9.351	11.0326	12.079	14.6894	11.3936	15.246	18.6127	15.9089	20.365	*52.0413*			
	T_f			23.9978			T_e			14.9159				
Ph10	η	66.6667	77.7778	75	46.1538	79.1667	64	76	80	83.3333	93.3333	80.7685%	41.1188%	60%
	α	***-76***	38.8889	39.7917	***-56.5385***	32.3264	***-71.8***	32.2333	35.0278	52.3611	51.1111			
	T	9.5345	12.8491	16.6834	12.3819	14.0774	***19.6582***	16.712	***21.4577***	13.2632	14.5473			
	T_f			17.875			T_e			14.6887				

Note: The reasons for experimental failures are highlighted in bold italics within the table, and the failed trials are marked in red font.

The system output parameters for the test 6 are detailed in Table 5, revealing a total of 6 transgressions, with 4 incidents recorded at Path2 (highlighted in bold). The system dynamically adjusts stimulation parameters including PF, UPN, PTN, and PA based on the current state vector $x = [e, e_c]$. The wireless neurostimulator generates real-time neuroelectric signals corresponding to these patterns, inducing varied behavioral responses in the pigeon robot. Instances, where the pigeon exhibits a substantial deviation and an escalating trend (points 1, 2, and 3 in Table 5), prompt the use of a stimulation mode involving PTN and multiple UPN. This aims to diminish the positional error while employing medium and low frequencies to curb the increasing trend in travel error. Conversely, when the pigeon experiences a slight deviation from the target path, and the changing trend favors error reduction (points 5 and 6 in Table 5), a stimulation mode with fewer PTN and UPN is applied. This correction aims to rectify the positional error, with medium or high frequencies refining the pigeon robot's behavior at the boundary.

Different from the drawbacks associated with the optimal parameter control method, which may result in excessive control of the pigeon robot, the control strategy proposed in this paper anticipates the pigeon robot's motion trend in the subsequent moment through the incorporation of the error rate of change e_c. Analyzing the system's tracking performance (refer to Fig. 7), we ascertain that this strategy adeptly suppresses the inclination for error escalation, thereby diminishing the frequency of stimuli. Importantly, the strategy demonstrates an absence of instances where the pigeon advances erratically along the target path, resembling the numeral "8". This process demonstrates its ability to track the target path in real-time using the optimal control parameters at each moment.

3.3. Performance of PAPTCS

The performance indicators of Ph1 are illustrated in Fig. 8. The experimental durations for the first and second trials, 43.6044s and 138.2109s respectively, exceed $2T_f$ and are thus excluded from performance analysis. The average error rate (α_e) in the PAPTCS's experiments is 36.7675%, signifying the system's proficiency in accurately tracking the target path. Control efficiencies (η) consistently exceed 70%, with an average control efficiency (η_e) of 74.0741%, coupled with an average experimental duration (T_e) of 15.4571s. These findings affirm the system's capability to efficiently track the target path while adhering to design specifications. The

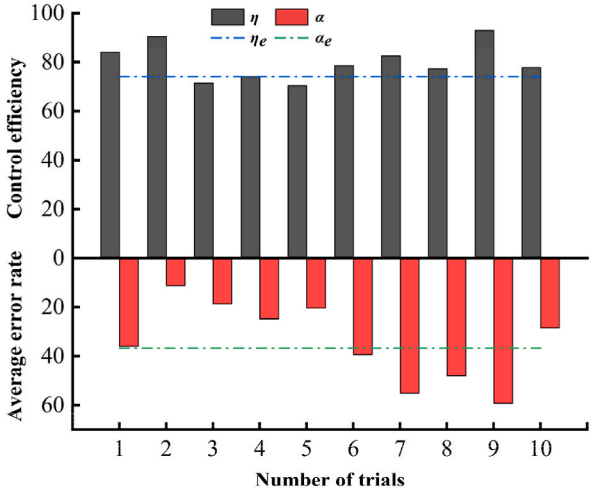

Fig. 8. Performance indicators of the control system.

system's design, encompassing a holistic consideration of error trend dynamics, successfully fulfills the control task of guiding the pigeon robot back to the target path without over-rotation, mitigating the occurrence of left and right folding back. Notably, the system adeptly avoids mismatches between distinct rotation requirements and optimal stimulus parameters. The results underscore the efficacy of the parameter adaptive control strategy, demonstrating its suitability for dynamically tracking the target path in the highly dynamic pigeon robot system, aligning seamlessly with moment-to-moment control demands.

ANOVA conducted on successful trials yielded non-significant differences between the control efficiency ($p = 0.675$, ANOVA) and the task average error rate ($p = 0.692$, ANOVA). These results suggest that an increase in the number of trials did not influence control performance. However, a noteworthy inter-individual significant difference emerged in task completion time ($p = 0.036$, ANOVA), highlighting a discernible individual effect on the task completion time for the tracking task.

Table 3 presents the statistical results of the control performance of the PAPTCS across all experiments. The reasons for experimental failures are highlighted in bold, and the failed trials are marked in red. The results indicate that the average error rate for all individuals was below the random chance level of 50%, with an average error rate of 37.24% across the five individuals. The system's average control efficiency was 82.17%. These findings demonstrate that the control system effectively avoids the "8" path and significantly enhances the performance of the pigeon robot in target path tracking.

4. Discussion

Electrical stimulation methods targeting sensory or motor brain areas are widely employed for the automatic control of animal robots. However, a challenge lies in dynamically selecting optimal stimulation parameters. To address this issue, this study proposes a parameter-adaptive path tracking control strategy for pigeon robots. Through the exploration of multiple sets of parameter levels, we identify combinations with minimal charge accumulation, thereby enhancing the overall stability of the control system. Notably, previous studies on automatic control of path tracking in animal robots lack research regarding parameter adaptation. Furthermore, there is a notable absence of research on the control of pigeon robots in open scenarios utilizing parameter adaptive control strategies.

4.1. Effect of different stimulation parameters on the control process

In pursuit of a stable, efficient, and enduring path tracking control system for pigeon robots, a comprehensive examination of various parameter levels and stimulus pattern combinations is imperative. This study systematically delves into and delineates the mapping relationship connecting independent variables of parameters to dependent variables of behavior. Subsequently, this mapping relationship is harnessed to devise adaptive strategies for parameter design.

Physiological studies on animals have demonstrated that lower stimulus frequencies are ineffective in activating neurons for excitation, while an appropriate frequency range induces behavioral responses in motor neurons [4–6]. Neurons involved in complex tasks or functional diversity typically exhibit a broader frequency range, while motor neurons dedicated to simpler or specific tasks have a narrower activation frequency spectrum [8]. High-frequency stimulation can induce sustained depolarization of nerve membranes, leading to a fatigue effect in neurons, and hindering their response to stimulus signals [48]. This study identified the pigeon robot's effective frequency range as 10–120 Hz. Amplitude exhibited no substantial increase at PF = 75 Hz compared to 100 Hz, despite significant differences in RA. The experiment revealed that increasing the frequency to 120 Hz did not result in higher RA and TD, prompting the designation of 100 Hz as the upper limit of the stimulation frequency (Fig. 6). Additionally, the pigeon robot exhibited no response to signals when PF < 20 Hz, while PF > 120 Hz led to noticeable body shaking and a stationary state, indicating the tolerated frequency upper limit. Consistent findings in previous research on rat motor cortex microstimulation parameters and

forelimb motor evoked potentials (MEP) support the notion of a fixed frequency range governing animal behavioral responses [44].

Generally, an escalation in PTN and UPN is associated with a concurrent rise in the number of directly activated neurons, likely contributing to the pronounced increase in RA and TD in the pigeon robot. Electrophysiological investigations have consistently demonstrated that the level of neuron activation is contingent upon the total effective charge applied to the brain [49]. As the charge magnitude increases, the neuroelectric signal duration prolongs, leading to a broader activation of neurons within the target brain area. Consequently, the response time of the animal's behavior extends, affording the pigeon ample time for processing externally applied conditioning information. This study further substantiates the mentioned finding by establishing a direct link between PTN and UPN increments and the heightened activation of neurons in the brain. This heightened neuronal activation emerges as the primary factor contributing to the substantial augmentation of rotation behavior. Notably, elevating PTN and UPN significantly enhances the likelihood of a shift in locomotor state. All pigeons transitioned to the walking state at the turn's conclusion when PTN exceeded 4 or UPN surpassed 5, marking the progression from static to dynamic continuous behavior (Table 2). Consequently, when orchestrating large-angle rotation in the pigeon robot's control process, the demand for continuous rotation control is met through diverse combinations of UPN and PTN.

Biological responses triggered by electrical nerve stimulation are intricately associated with the phenomenon of neuronal depolarization. The cathodic precursor's stimulus pulse waveform induces an efflux of intracellular positive charge, diminishing the cell membrane potential and prompting neural tissue excitation. External electrical stimulation, for inducing neural excitation, necessitates a pulse amplitude surpassing the action potential's minimum threshold. The action thresholds of all individuals, except for the Ph2 right FRM, exceeded 0.2 mA in this study. Following initial stimulation, cells rapidly enter an excited state, with their excitability enduring for a defined duration [50,51]. Larger amplitudes expedite ion flow rates both inside and outside the cell, activating deeper neuronal cells. This acceleration constitutes the primary reason for the abbreviated response time in rotation behavior. The study demonstrates that surpassing the maximum threshold ($PA_{max} = 0.4$ mA) significantly disrupts the pigeon's body balance, emphasizing that PA is not optimally applied to control the behavior of pigeon robots (Fig. 6l; Table 2).

In the behavioral analysis of the pigeon robots, significant variations in rotation angles were observed among different stimulus parameter levels and, in specific instances (e.g., UPN and PA parameters of Ph1), between travel distances. This outcome indicates that the FRM predominantly performs neural activities associated with body rotation, with alterations in travel distance representing a consequential adaptation to body rotation. Notably, a majority of individuals ($n = 4$) exhibited a more pronounced left-turn response compared to right-turn responses. Based on previous research [52], functional differences have been identified between the left and right brain regions of pigeons: the left hemisphere is primarily involved in spatial tasks, while the right hemisphere excels in processing social information. The behavioral tasks of rotational control and path tracking in this study fall within the category of spatial tasks. Under conditions where frequency or amplitude is varied, the advanced neural pathways associated with the left hemisphere's behavioral responses may result in more pronounced leftward turning responses compared to rightward turning. However, changes in other parameters did not exhibit significant differences in their effects between the left and right brain regions.

Under the experimental conditions, a strong positive correlation between RA (rotation angle) and TD (travel distance) was observed for both the left and right sides. This indicates that as stimulation parameters increase RA, TD also increases correspondingly, and vice versa. Overall, the correlation on the right side was found to be stronger and more significant compared to the left side (with right-side correlation coefficients exceeding 0.95 and p-values less than 0.05 across all experimental conditions), suggesting that individual behavioral responses under right-side stimulation are more consistent.

In the frequency adjustment experiments, the correlation between RA and TD was significant on the right side ($r = 0.99$, $p = 0.013$), while a strong correlation was observed on the left side but was not statistically significant ($r = 0.89$, $p = 0.11$). In experiments involving the number of pulses (UPN/Size) and pulse trains (PTN/String), both sides exhibited significant positive correlations, particularly on the right side ($r > 0.95$), indicating that these parameters have a consistent impact on motor behavior across both sides. The effect of amplitude (PA/mA) variations on RA and TD showed a very strong correlation on both sides ($r > 0.98$, $p < 0.05$), with a particularly strong correlation on the left side ($r = 0.99$, $p = 0.007$), demonstrating that amplitude variations can precisely control the individual's motor responses.

The outcomes of this study align with observations from the rat robot, wherein animals exhibited abrupt rotation motions in response to high-amplitude stimuli. The animals concluded their response within a duration of 3–4s following stimulus application. After the cessation of the stimulus pulse, neurons gradually returned to the resting state within a timeframe of 1.5–2.5s [11]. Building upon these findings, this paper adopts a neuromodulation pulse duty cycle of 1/3 and maintains a fixed unit pulse interval of 100 ms. This choice not only prevents overexcitation, thereby averting the emergence of a refractory period in the target nucleus [53] but also ensures sustained neuron excitability over a defined duration.

Stimulation patterns exert a direct influence on the extent of motion response and the transition between behavioral states in pigeon robots. The animal motor conditioning system selectively engages distinct functional subareas of the FRM and specific motor neural pathways to accommodate rotation requirements in varying rotation scenarios. The wireless neurostimulator generates diverse neuromodulation pulses targeting the designated brain area. This diversity in stimulation modes serves to prolong the brain's tolerance, ensuring sustained system efficacy over the long term. Furthermore, it enhances the system's capacity to control pigeon behavior [17,37,42].

Overall, the behavioral patterns of the five individuals under different stimulation conditions showed a high degree of consistency, suggesting that the research results are both replicable and reliable. The stable patterns observed across different stimulation parameters provide a solid foundation for further development of neural control systems.

4.2. Performance analysis of PAPTCS

To attain a specific control objective, the design of diverse stimulus patterns is imperative to concurrently elicit desired physiological responses, such as inducing visual perception, generating limbic behaviors, or facilitating a specific task. These responses manifest externally and internally, characterized by factors such as the rate of activation, the volume of activated tissues, and the duration. Effective control over these effects is achievable through the control of microelectrical stimulation parameters. Traditionally, optimal stimulation parameters are selected as the control system output based on an individual's response characteristics to pulse parameters. However, this approach fails to meet the precise control requirements for tracking the target path during the system's operation. The primary reason is that biological behavior is influenced by multiple factors, resulting in a non-linear relationship between parameters and behavioral responses, with significant variations among individuals. Additionally, path tracking is a highly dynamic and real-time task that demands the control system to possess self-adjusting capabilities. Fuzzy control principles can simulate the response of different individuals to parameters and generate stimulation patterns that meet the real-time requirements for precise path tracking. This approach allows for pre-control of boundary behaviors, resulting in smoother trajectories for the pigeon robots and preventing the occurrence of "8" paths.

The results of this study reveal that the control success rate exceeds 80% for most individuals, except for individual Ph10, and notably achieving 90% for Ph2. The average error rate in experiments is predominantly below 50%, highlighting the impracticality of pursuing full controllability akin to mechanical robots for animal counterparts like pigeon robots, which possess intrinsic cognitive processes. The design of control strategies for animal robots should align with the external environment of creatures and intentions. Moreover, the average control efficiencies in experiments consistently fall within the efficient control range, reaching an impressive 93.1577% for Ph7. This indicates that the behavioral decisions of the pigeon robot can be effectively influenced through applied neuroelectric stimulation, facilitating the execution of desired actions and the successful accomplishment of tasks specified by human operators.

In contrast to prior investigations [35–37,39], where the prevalent "8" path was frequently observed, the incorporation of the positional error trend in our study facilitated a proactive adjustment of the pigeon's motion direction. This adjustment was achieved through the application of stimulus parameters featuring a gentle control effect, effectively curbing the pigeons' inclination to persist in an incorrect path via a frequency reduction approach. Notably, the stimulus amplitude was identified as a crucial factor inducing drastic changes in response behavior during rotation adjustments. Consequently, our parameter adaptive strategy prioritized a low amplitude as the foundational parameter, complemented by the utilization of diverse stimulus modes for effective neuromodulation signaling.

The difficulty of the control process may be influenced by multiple factors. Research indicates that an individual's age and cognitive level can affect behavioral responses. In studies on locusts, older locusts typically respond more quickly to threats than younger ones, which helps to explain instances of control failure observed in the early stages of experiments [54]. At the beginning of the experiments, pigeons exhibited a preference for specific routes that aligned with their natural movement patterns, due to their familiarity with the experimental environment. This behavior is well-documented in homing pigeon studies, where pigeons tend to adhere to established routes even when faced with unforeseen disruptions, such as predators [55] or multiple release points. This tendency may account for the control challenges encountered during the task adaptation phase, as shown in Fig. 7, where the pigeons' innate movement intentions might interfere with effective task control. Additionally, individual pigeons display varying personality traits. More bold individuals exhibit greater openness, are more receptive to new stimuli, and have a stronger exploratory inclination. In contrast, more introverted pigeons may be resistant to altering their established paths when subjected to external control commands [56]. These factors contribute to hesitancy in some individuals during effective target path tracking, thereby reducing the overall success rate.

Using controllable biological robots for biological research enables the simulation of most scenarios required by researchers while avoiding the species rejection responses commonly encountered in mechanical robot simulations. This approach is of significant importance for a deeper understanding of animal social interactions, spatial cognition, and navigation [57]. The findings of this study hold practical significance in advancing the fine control of biological robot behavior. By combining specific rules and stimulation patterns, this research has achieved pre-control and fine-tuning of biological robot behavior, successfully overcoming the previously common issue of "8"-shaped travel paths. Moreover, the proposed parameter-adaptive control strategy allows for dynamic adjustment of stimulation parameter combinations based on actual control requirements, making the control more flexible and providing a replicable method for the neural regulation of biological robots.

This study also promotes interdisciplinary research across fields such as biology, robotics, biomedicine, and environmental science. For instance, robotic rehabilitation systems enable precise control to deliver repetitive motion training while minimizing human error. Neurostimulation technologies, such as deep brain stimulation (DBS) and transcranial magnetic stimulation (TMS), directly activate the nervous system to facilitate neurorepair and neuroplasticity, aiding in the recovery of motor function. Combining neurostimulation with robotic rehabilitation allows for dynamic adjustment of therapeutic parameters based on patient needs, enhancing the effectiveness of personalized rehabilitation [58].

Additionally, the use of controllable biological robots in biological research enables the simulation of most experimental scenarios while avoiding the species rejection reactions often encountered in mechanical robot simulations. This approach also reduces the uncertainty and variability introduced by live animals in traditional experiments, thereby improving the reproducibility and accuracy of research[59,60]. Such advancements are of great significance in gaining a deeper understanding of animal social interactions, spatial cognition, and navigational behavior, ultimately contributing to the design of more natural and effective biological robot systems.

5. Limitations of the study

Neural electrical stimulation offers significant advantages in controlling animal robots, providing essential technical means for research in animal robot behavior control. This study validates the feasibility of the pigeon robot path tracking control system from a system design perspective and demonstrates the system's effectiveness on the ground. In the design of automatic control systems for flight-capable biological robots, although strategies for controlling specific behaviors through the intervention of pigeon intentions have been successfully implemented in laboratory settings, external environmental effects on pigeon movement intentions have not been considered due to the limited number of experiments and individual differences. Additionally, there is a lack of feedback mechanisms related to the awareness of the biological entities.

Future research should focus on integrating the intrinsic behavioral intentions of animals with human interventions to design more effective control systems at the level of animal intentions. Additionally, due to the inherent challenges in interpreting subjective experiences of animals, humans typically rely on observable behaviors and physiological responses to assess emotional expression. Therefore, a deeper investigation into the control mechanisms of emotion-related neural clusters and the subjective perception of external stimuli will significantly advance our understanding of the complex mechanisms of neural regulation.

CRediT authorship contribution statement

Yinggang Huang: Writing – review & editing, Writing – original draft, Validation, Software, Methodology, Investigation, Formal analysis, Data curation, Conceptualization. **Lifang Yang:** Software, Formal analysis. **Long Yang:** Validation, Data curation. **Zehua Xu:** Visualization, Validation. **Mengmeng Li:** Writing – review & editing, Supervision, Project administration, Funding acquisition, Data curation, Conceptualization. **Zhigang Shang:** Writing – review & editing, Supervision, Resources, Project administration, Methodology, Investigation, Conceptualization.

Declaration of competing interest

The authors declare that they have no known competing financial interests or personal relationships that could have appeared to influence the work reported in this paper.

Acknowledgments

This work was supported by the National Natural Science Foundation of China (62301496), the Postdoctoral Fellowship Program of China Postdoctoral Science Foundation (GZC20232447), the Program for Science and Technology of Henan Province of China (242300421411) and the STI 2030-Major Project (2022ZD0208500). Our deepest gratitude goes to the anonymous reviewers and editors for their careful work and thoughtful suggestions that have helped improve this paper substantially.

References

[1] Z. Gao, Q. Shi, T. Fukuda, C. Li, Q. Huang, An overview of biomimetic robots with animal behaviors, Neurocomputing 332 (2019) 339–350. https://doi.org/10.1016/j.neucom.2018.12.071.
[2] D. Romano, E. Donati, G. Benelli, et al., A review on animal-robot interaction: from bio-hybrid organisms to mixed societies, Biol. Cybern. 113 (3) (2019) 201–225. https://doi.org/10.1007/s00422-018-0787-5.
[3] S. Yun, C.S. Koh, J. Jeong, et al., Remote-controlled fully implantable neural stimulator for freely moving small animal, Electronics 8 (6) (2019) 706. https://doi.org/10.3390/electronics8060706.
[4] S.J. Chang, A.J. Santamaria, F.J. Sanchez, et al., Deep brain stimulation of midbrain locomotor circuits in the freely moving pig, Brain Stimul. 14 (3) (2021) 467–476. https://doi.org/10.1016/j.brs.2021.02.017.
[5] I. Opris, X. Dai, D.M.G. Johnson, et al., Activation of brainstem neurons during mesencephalic locomotor region-evoked locomotion in the cat, Front. Syst. Neurosci. 13 (2019) 69. https://doi.org/10.3389/fnsys.2019.00069.
[6] L.C. Bachmann, A. Matis, N.T. Lindau, et al., Deep brain stimulation of the midbrain locomotor region improves paretic hindlimb function after spinal cord injury in rats, Sci. Transl. Med. 5 (208) (2013) 208ra146. https://doi.org/10.1126/scitranslmed.3005972.
[7] C. Kong, J. Shin, C.S. Koh, et al., Optimization of medial forebrain bundle stimulation parameters for operant conditioning of rats, Stereotact. Funct. Neurosurg. 97 (1) (2019) 1–9. https://doi.org/10.1159/000497151.
[8] M. Jamali, Y. Jamali, M. Golshani, Theory of cyborg: a new approach to fish locomotion control, arXiv (USA) (2019) 22–29 [Online]. http://arxiv.org/abs/1904.12460.
[9] K. Hirao, M. Ariyanto, Y. Fujita, et al., Heat source approaching by cyborg cockroach using a new antennae electrode implantation method, in: 2022 International Symposium On Micro-NanoMehatronics And Human Science (MHS), 2022, pp. 1–6, https://doi.org/10.1109/mhs56725.2022.10092120. Nagoya, Japan.
[10] R. Huai, H. Zhu, S. Yang, et al., Trajectory recording and analysis system for cockroach robot, bioRxiv (2021). https://doi.org/10.1101/2021.11.16.468890.
[11] J.C. Erickson, M. Herrera, M. Bustamante, et al., Effective stimulus parameters for directed locomotion in Madagascar hissing cockroach biobot, PLoS One 10 (8) (2015) e0134348, https://doi.org/10.1371/journal.pone.0134348.
[12] Dong M., Cai L., Wang H., et al., A preliminary study on motion eliciting by electrically stimulating midbrain of pigeon, J. Biol. 29 (4) (2012) 33–35. (In Chinese).
[13] Z. Zhou, H. Mei, R. Li, et al., Progresses of animal robots: a historical review and perspectiveness, Heliyon 8 (11) (2022) e11499.
[14] N. Kobayashi, M. Yoshida, N. Matsumoto, et al., Artificial control of swimming in goldfish by brain stimulation: confirmation of the midbrain nuclei as the swimming center, Neurosci. Lett. 452 (1) (2009) 42–46. https://doi.org/10.1016/j.neulet.2009.01.035.
[15] L. Cai, Z. Dai, W. Wang, et al., Modulating motor behaviors by electrical stimulation of specific nuclei in pigeons, JBE 12 (4) (2015) 555–564. https://doi.org/10.1016/s1672-6529(14)60145-1.
[16] J. Jang, C. Baek, S. Kim, et al., Current stimulation of the midbrain nucleus in pigeons for avian flight control, Micromachines 12 (7) (2021) 788. https://doi.org/10.3390/mi12070788.

[17] H. Wang, J. Li, L. Cai, et al., Flight control of robo-pigeon using a neural stimulation algorithm, J. Integr. Neurosci. 17 (4) (2018) 337–342. https://doi.org/10.31083/j.jin.2018.04.0413.
[18] J.Q. Yang, R. Huai, H. Wang, et al., Global positioning system-based stimulation for robo-pigeons in open space, Front. Neurorob. 11 (8) (2017) 40, https://doi.org/10.3389/fnbot.2017.00040.
[19] J. Seo, G.J. Choi, S. Park, et al., Wireless navigation of pigeons using polymer-based fully implantable stimulator: a pilot study using depth electrodes, 2017, Korea (South) (2017) 917–920.
[20] G.J. Choj, J. Jang, S. Kim, et al., A fully implantable wireless stimulation system for pigeon navigation, in: 2019 41st Annual International Conference of the IEEE Engineering in Medicine and Biology Society (EMBC), 2019, pp. 5310–5313. Berlin, Germany.
[21] X. Liu, Z. Su, Q. Gao, et al., Wireless-controlled cubic neural stimulator for free-moving animals, R. Soc. Open Sci. 10 (3) (2023) 221116. https://doi.org/10.1098/rsos.221116.
[22] S. Shim, S. Yun, S. Kim, et al., A handheld neural stimulation controller for avian navigation guided by remote control, Bio Med. Mater. Eng. 30 (5–6) (2020) 497–507, https://doi.org/10.3233/BME-191070.
[23] F. Velasco, P.E. Saucedo-Alvarado, D. Vazquez-Barron, et al., Deep brain stimulation for refractory temporal lobe epilepsy. Current status and future trends, Front. Neurol. 13 (2022) 796846. https://doi.org/10.3389/fneur.2022.796846.
[24] G. Kozák, A. Berényi, Sustained efficacy of closed loop electrical stimulation for long-term treatment of absence epilepsy in rats, Sci. Rep. 7 (2017) 6300. https://doi.org/10.1038/s41598-017-06684-0.
[25] J. Selvaraj, P. Rastogi, N.P. Gaunkar, et al., Transcranial magnetic stimulation: design of a stimulator and a focused coil for the application of small animals, IEEE Trans. Magn. 54 (11) (2018) 5200405. https://doi.org/10.1109/tmag.2018.2846521.
[26] J.T. Paz, T.J. Davidson, E.S. Frechette, et al., Closed-loop optogenetic control of thalamus as a tool for interrupting seizures after cortical injury, Nat. Neurosci. 16 (1) (2013) 64–70. https://doi.org/10.1038/nn.3269.
[27] K. Zhao, H. Wan, Z. Shang, et al., Intracortical microstimulation parameters modulate flight behavior in pigeon, J. Integr. Neurosci. 18 (1) (2019) 23–32. https://doi.org/10.31083/j.jin.2019.01.14.
[28] J.C. Lilly, J.R. Hughes, E.C. Alvord Jr., et al., noninjurious electric waveform for stimulation of the brain, Science 121 (3144) (1955) 468–469. https://doi.org/10.1126/science.121.3144.468.
[29] H.D. Nguyen, P.Z. Tan, H. Sato, et al., Sideways walking control of a cyborg beetle, IEEE T. Med. Robot. Bio. 2 (3) (2020) 331–337. https://doi.org/10.1109/tmrb.2020.3004632.
[30] H. Siljak, P.H.J. Nardelli, R.C. Moioli, Cyborg insects: bug or a feature? IEEE Access 10 (2022) 49398–49411. https://doi.org/10.1109/access.2022.3172980.
[31] Y. Lee, S. Kim, Y.K. Cho, et al., Amygdala electrical stimulation for operant conditioning in rat navigation, Biomed. Eng. Lett. 14 (2) (2024) 291–306. https://doi.org/10.1007/s13534-023-00336-1.
[32] J. Huo, L. Zhang, X. Luo, et al.,, Motor behavior regulation of rat robots using integrated electrodes stimulated by micro-nervous system, Micromachines 15 (5) (2024) 587. https://doi.org/10.3390/mi15050587.
[33] Y. Zhao, Y. Peng, Y. Wen, et al., A novel movement behavior control method for carp robot through the stimulation of medial longitudinal fasciculus nucleus of midbrain, JBE 19 (5) (2022) 1302–1313. https://doi.org/10.1007/s42235-022-00211-2.
[34] D.R. Merrill, M. Bikson, J.G.R. Jefferys, Electrical stimulation of excitable tissue: design of efficacious and safe protocols, J. Neurosci. Methods. 141 (2) (2005) 171–198. https://doi.org/10.1016/j.jneumeth.2004.10.020.
[35] R. Huai, J. Yang, H. Wang, The robo-pigeon based on the multiple brain regions synchronization implanted microelectrodes, Bioengineered 7 (4) (2016) 213–218. https://doi.org/10.1080/21655979.2016.1197033.
[36] H. Wang, J. Yang, C. Lv, et al., Intercollicular nucleus electric stimulation encoded “walk forward” commands in pigeons, Anim. Biol. Leiden. 68 (2) (2018) 213–225. https://doi.org/10.1163/15707563-17000053.
[37] J. Yang, R. Huai, H. Wang, et al., A robo-pigeon based on an innovative multi-mode telestimulation system, Bio Med. Mater. Eng. 26 (S1) (2015) S357–S363, https://doi.org/10.3233/BME-151323.
[38] K. Fang, H. Mei, Y. Tang, et al., Grade-control outdoor turning flight of robo-pigeon with quantitative stimulus parameters, Front. Neurorob. 17 (2023) 1143601. https://doi.org/10.3389/fnbot.2023.1143601.
[39] Z. Zhou, D. Liu, H. Sun, et al., Pigeon robot for navigation guided by remote control: system construction and functional verification, JBE 18 (1) (2021) 184–196. https://doi.org/10.1007/s42235-021-0013-3.
[40] M. Deprez, K. Luyck, L. Luyten, et al., An evaluation of the effect of pulses-hape on grey and white matter stimulation in the rat brain, Sci. Rep. 8 (2018) 752. https://doi.org/10.1038/s41598-017-19023-0.
[41] E.J. Tehovnik, Electrical stimulation of neural tissue to evoke behavioral responses, J. Neurosci. Methods. 65 (1) (1996) 1–17. https://doi.org/10.1016/0165-0270(95)00131-x.
[42] R. Yan, Z. Qiu, Z. Chen, et al., A wireless animal robot stimulation system based on neuronal electrical signal characteristics, in: 2023 IEEE 3rd International Conference on Information Technology, Big Data and Artificial Intelligence (ICIBA), Chongqing, China, 2023, pp. 244–249.
[43] H. Xu, H. Xie, Y. Chen, et al., A new cyborg rat auto navigation system based on finite state machine, IEEE Sensor. J. 23 (19) (2023) 23456–23466. https://doi.org/10.1109/jsen.2023.3291870.
[44] M. Watson, N. Dancause, M. Sawan, Intracortical microstimulation parameters dictate the amplitude and latency of evoked responses, Brain Stimul. 9 (2) (2016) 276–284. https://doi.org/10.1016/j.brs.2015.10.008.
[45] S.N. Margalit, H. Slovin, Spatio-temporal characteristics of population responses evoked by microstimulation in the barrel cortex, Sci. Rep. 8 (2018) 13913. https://doi.org/10.1038/s41598-018-32148-0.
[46] L. He, X. Cheng, A. Jiwa, et al., Zanthoxylum bungeanum fruit detection by adaptive thresholds in HSV space for an automatic picking system, IEEE Sensor. J. (2023) 14471–14486. https://doi.org/10.1109/jsen.2023.3277042.
[47] N.M. Laird, F. Mosteller, Some statistical methods for combining experimental results, Int. J. Technol. Assess. 6 (1) (1990) 5–30.
[48] D.S. Shin, M. Samoilova, M. Cotic, et al., High frequency stimulation or elevated K+ depresses neuronal activity in the rat entopeduncular nucleus, Neuroscience 149 (1) (2007) 68–86. https://doi.org/10.1016/j.neuroscience.2007.06.055.
[49] J. Yeomans, P. Prior, F. Bateman, Current-distance relations of axons mediating circling elicited by midbrain stimulation, Brain Res. 372 (1) (1986) 95–106. https://doi.org/10.1016/0006-8993(86)91462-9.
[50] E.A. DeYoe, J.D. Lewine, R.W. Doty, Laminar variation in threshold for detection of electrical excitation of striate cortex by macaques, J. Neurophysiol. 94 (5) (2005) 3443–3450. https://doi.org/10.1152/jn.00407.2005.
[51] J.R. Bartlett, E.A. DeYoe, R.W. Doty, et al., Psychophysics of electrical stimulation of striate cortex in macaque, J. Neurophysiol. 94 (5) (2005) 3430–3442. https://doi.org/10.1152/jn.00406.2005.
[52] M. Nagy, Z. Ákos, D. Biro, et al., Hierarchical group dynamics in pigeon flocks, Nature 464 7290 (2010) 890–893.
[53] D.M. Atrens, D.M. Cobbin, Ipsiversive rotation elicited by electrical stimulation of the mesencephalon: an analysis of intracranial electrical stimulation parameters and refractory periods, Exp. Neurol. 53 (2) (1976) 314–327. https://doi.org/10.1016/0014-4886(76)90074-1.
[54] D. Romano, J. Bloemberg, M. Tannous, et al., Impact of aging and cognitive mechanisms on high-speed motor activation patterns: evidence from an orthoptera-robot interaction, IEEE T. Med. Robot. Bio. 2 (2) (2020) 292–296. https://doi.org/10.1109/tmrb.2020.2977003.
[55] T. Guilford, D. Biro, Route following and the pigeon’s familiar area map, J. Exp. Biol. 217 (2) (2014) 169–179. https://doi.org/10.1242/jeb.092908.
[56] T. Sasaki, R.P. Mann, K.N. Warren, et al., Personality and the collective: bold homing pigeons occupy higher leadership ranks in flocks, Phil. Trans. Biol. Sci. 373 (2018) 20170038. https://doi.org/10.1098/rstb.2017.0038.
[57] A. Frohnwieser, J.C. Murray, T.W. Pike, et al., Using robots to understand animal cognition, J. Exp. Anal. Behav. 105 (1) (2016) 14–22. https://doi.org/10.1002/jeab.193.

[58] Z.Z. Major, C. Vaida, K.A. Major, et al., The impact of robotic rehabilitation on the motor system in neurological diseases. A multimodal neurophysiological approach, Int. J. Environ. Res. Publ. Health. 17 (18) (2020) 6557. https://doi.org/10.3390/ijerph17186557.
[59] D. Romano, G. Benelli, C. Stefanini, et al., How aggressive interactions with biomimetic agents optimize reproductive performances in mass-reared males of the Mediterranean fruit fly, Biol. Cybern. 117 (3) (2023) 249–258. https://doi.org/10.1007/s00422-023-00965-w.
[60] F. Ladu, V. Mwaffo, J. Li, et al., Acute caffeine administration affects zebrafish response to a robotic stimulus, Behav. Brain Res. 289 (2015) 48–54. https://doi.org/10.1016/j.bbr.2015.04.020.